https://doi.org/10.5194/egusphere-2026-1507
Preprint. Discussion started: 24 March 2026

Coastal Eddies as Vectors for Connectivity During the Summer in the Levantine Sea

Yotam Fadida[1,2], Tal Ozer[1], Tal Ben Ezra[3], Michael D. Krom[3,4], Anat Tsemel[3], Tatiana Margo Tsagaraki[5], Eli Biton[1], Yaron Toledo[6], and Yoav Lehahn[2]

[1]Israel Oceanographic and Limnological Research, Haifa, Israel
[2]Department of Marine Geosciences, Leon H. Charney School of Marine Sciences, University of Haifa, Haifa, Israel
[3]Morris Kahn Marine Research Station, Department of Marine Biology, Leon H. Charney School of Marine Sciences, University of Haifa, Haifa, Israel
[4]School of Earth and Environment, University of Leeds, Leeds, UK
[5]Department of Biological Sciences, University of Bergen, Bergen, Norway
[6]School of Mechanical Engineering, Tel-Aviv University, Tel-Aviv-Yafo, Israel

Correspondence: Yoav Lehahn (ylehahn@univ.haifa.ac.il), Yotam Fadida (yotam@ocean.org.il)

Abstract. The Levantine Basin, the easternmost part of the Mediterranean Sea, is one of the most oligotrophic marine environments worldwide. A pronounced gradient separates its relatively chlorophyll-enriched coastal zone from the severely depleted offshore waters, and the degree of connectivity between these regions shapes the distribution of biomass and nutrients. The connectivity between these two contrasted regimes is highly seasonal: during winter, deep mixing and enhanced lateral stirring promote basin-wide exchange, whereas in summer, strong stratification and a persistent alongshore current largely suppress cross-shore transport. Here we examine how the limited summertime connectivity is affected by coastal mesoscale eddies, which are a recurring features in this region. This is done through analysis of satellite imagery, autonomous glider transects, high-frequency (HF) radar measurements, and cruise-based nutrient profiles. Our observations show that these eddies can export considerable amounts of coastal biomass into offshore waters. The sampled eddies exhibited elevated surface chlorophyll and sea surface temperatures (SST), enhanced surface silica and inorganic particulate matter concentrations, and a shoaling and broadening of the deep chlorophyll maximum (DCM), all indicative of coastal origins. HF radar observations further revealed dynamically coherent anticyclonic circulation, supporting their role as active transport features rather than passively advected surface patches. Our results demonstrate that coastal mesoscale eddies transport coastal water and their biogeochemical signatures into the open Levantine Basin. These findings establish coastal mesoscale eddies as episodic, yet significant contributors to summer cross-shore exchange in one of the world's most oligotrophic marine regions.

1 Introduction

The Eastern Mediterranean Sea (EMS), particularly its easternmost sub-basin, the Levantine Basin, is among the most oligotrophic marine environments on Earth (Krom et al., 2005, 2014; Psarra et al., 2000). Extremely low nutrient concentrations and correspondingly low primary productivity are defining characteristics of its offshore waters (Kress and Herut, 2001; Moutin et al., 2012; Pujo-Pay et al., 2011). Within this generally nutrient-depleted setting, a cross-shore gradient exists between the

https://doi.org/10.5194/egusphere-2026-1507
Preprint. Discussion started: 24 March 2026

coastal region—where sediment-water interactions and terrestrial inputs can moderately enhance nutrient availability, chlorophyll concentrations, and primary production (Azov, 1986; Berman et al., 1984; Nixon, 2003; Krom et al., 2004; Kress and Herut, 1998; Raveh et al., 2015; Herut et al., 1999)—and the ultra-oligotrophic offshore waters (Crombet et al., 2011; Zohary and Robarts, 1998; Ignatiades et al., 2009). Although this contrast is weaker than in many other boundary systems (Ben-Ezra et al., 2023), it remains an important element of the basin's ecological structure (Reich et al., 2022; Herut et al., 2000; Raveh et al., 2015).

Exchanges between the coastal and offshore domains influence nutrient supply, primary production, and ecosystem functioning across the Levantine Basin (Ribera d'Alcalà et al., 2003; Siokou-Frangou et al., 2010). Periods of enhanced connectivity can transport biomass and nutrient-enriched waters offshore (Barale et al., 2008; Alkalay et al., 2020; Katz et al., 2020), while reduced connectivity leaves the offshore region effectively isolated. The efficiency and pathways of this coastal–offshore exchange, therefore, play a central role in shaping regional biogeochemical variability.

Connectivity in the EMS exhibits strong seasonality (Estrada, 1996; Rosentraub and Brenner, 2007). During winter, vertical mixing deepens the mixed layer and injects nutrients into the euphotic zone (Siokou-Frangou et al., 2010; Barale et al., 2008), while submesoscale instabilities enhance lateral stirring (Lévy et al., 2012). Recent work indicates that such wintertime horizontal processes contribute substantially to the seasonal offshore chlorophyll increase (Fadida et al., 2026). These findings emphasize the role of small-scale dynamics in regulating offshore enrichment during the winter.

In contrast, during the more stratified summer conditions, the connectivity regime changes markedly. Strong stratification suppresses vertical nutrient resupply, while the persistent alongshore current limits cross-shore exchanges, effectively decoupling the coastal zone from the offshore basin (Ozer et al., 2022; Verma et al., 2024; Akpınar, 2024). As a result, offshore waters remain extremely nutrient-poor, and coastal signals are typically confined nearshore. As such, any mechanisms capable of intermittently bridging the coastal–offshore divide during summer are of particular interest, even if their overall contribution is episodic or spatially limited.

Mesoscale features such as coastal eddies and filaments are frequently observed along the Levantine coast during summer (Menna et al., 2012; Estournel et al., 2021; Efrati et al., 2013). Their formation has been attributed to wind-driven current separation, mesoscale instabilities, and bathymetric deflection of the coastal jet, as documented by high-resolution models, in situ observations, and satellite analyses (Akpınar, 2024; Gerin et al., 2009; Verma et al., 2024; Baaklini et al., 2024). While these structures are known to extend offshore and advect surface tracers (Gertman et al., 2010; Martin, 2003; Flos and Tintoré, 1990), their role in coastal–offshore exchange under summer stratification remains uncertain. During this season, the Levantine Basin is characterized by strong vertical stratification, extremely low surface nutrient concentrations, and a pronounced deep chlorophyll maximum (DCM) near the nutricline (Mignot et al., 2014; Teruzzi et al., 2021; Ediger and Yilmaz, 1996; Ben-Ezra et al., 2024). In other stratified coastal systems, mesoscale eddies have been shown to reorganize surface chlorophyll, DCM, and the nutrient field under stratified conditions (Cornec et al., 2021; Wang et al., 2018; Espinosa-Carreón et al., 2012; Xu et al., 2023). Although surface expressions of coastal eddies in the Levantine Basin have been documented using satellite and in situ observations (Efrati et al., 2013; Baaklini et al., 2024), their impact on the vertical biogeochemical structure of the water column remains unquantified.

https://doi.org/10.5194/egusphere-2026-1507
Preprint. Discussion started: 24 March 2026

In this study, we investigate the role of coastal mesoscale eddies and filaments as episodic pathways for summer cross-shelf exchange in the eastern Levantine Basin. Combining satellite-derived chlorophyll fields, HF radar surface currents, autonomous glider transects, and ship-based nutrient, major element particulate matter geochemistry and chlorophyll profiles, we identify coherent coastal features and characterize their propagation, kinematics, and three-dimensional hydrographic and biogeochemical structure. By comparing conditions within these features to the surrounding offshore background, we show that they transport a distinct coastal water-mass signature offshore, characterized by a shoaled DCM, elevated surface and subsurface chlorophyll, and enhanced nutrient concentrations. Our results provide the first observational evidence that coastal mesoscale eddies and filaments can intermittently disrupt the summertime coastal–offshore separation in one of the world's most oligotrophic marine regions.

2 Data and Methods

2.1 Data

2.1.1 Satellite data.

This study was conducted using E.U. Copernicus Marine Service Information; DOI: 10.48670/moi-00300. Estimation of the mass concentration of chlorophyll-a in seawater (CHL) was derived from the gridded L4 daily ocean-color (1/100 degrees spatial resolution) data set. Data from several satellite missions (SeaWiFS, MODIS, MERIS, VIIRS-SNPP and JPSS1, OLCI-S3A) are combined to provide interpolated gap-free data sets (Volpe et al., 2018), using region-specific algorithms (Case-1 waters (Volpe et al., 2019), with new coefficients; and Case-2 waters (Berthon and Zibordi, 2004)). The images where all taken approximately at 13:00, which is generally when the satellite passes over the region.

Geostrophic currents were estimated using the Copernicus altimeter satellite gridded Sea Level Anomalies (SLA) computed with respect to a twenty-year [1993, 2012] mean DOI: 10.48670/moi-00142. A gridded L4 product with a spatial resolution of 1/8 degrees.

Sea Surface Temperature (SST) was estimated with the Copernicus Ultra High Resolution Sea Surface Temperature Analysis product DOI: doi.org/10.48670/moi-00172. A L4 gridded product with a spatial resolution of 1/100 degrees.

2.1.2 Glider Data

An autonomous underwater vehicle (SeaExplorer glider, Alseamar) equipped with a fluorometer by WetLabs and a CTD (conductivity, temperature, depth) by Sea-Bird was deployed for a variety of missions between the years 2018-2023. The missions (M141, M164) that coincided with summertime coastal eddies were analyzed for this study. The glider collected CTD and fluorescence data at very high spatiotemporal coverage through the upper 700 m of the water column. 360 dives were utilized from M141's mission in June/July 2018, yielding a 118 km transect (repeated twice). 55 dives where utilized from M164's mission in June 2022, yielding an 85 km transect. Glider dives, horizontally spaced at 3 km intervals, were separated into descending and ascending profiles and treated as quasi-vertical measurements (1.5 km apart).

https://doi.org/10.5194/egusphere-2026-1507
Preprint. Discussion started: 24 March 2026

2.1.3 High Frequency Radar

The Israeli coastal HF-radar network, operated by the Marine Engineering and Physics Laboratory at Tel Aviv University, consists of two WERA (WavE Radar; (Gurgel et al., 1999)) systems located at Ashkelon and Ashdod along the southeastern Mediterranean coast (Lorente et al., 2022). Each station operates in a monostatic configuration with co-located transmit and 12-element receive arrays, transmitting at a central frequency of 8.3 MHz and providing radial current coverage of up to approximately 180 km, depending on environmental conditions (Crombie, 1955; Barrick, 1977; Wyatt, 1991). The two sites are separated by roughly 25-km to optimize the overlap of their radial coverage for wave measurements (Hasselmann, 1971; Gurgel et al., 2006). This relatively close spacing ensures sufficiently large crossing angles between the two radar beams in the near field, improving the conditioning of directional inversions and enhancing the reliability of derived wave spectra. At the same time, the configuration constrains the region of robust two-dimensional current and wave mapping to about 75-km offshore, beyond which geometric dilution and weaker second-order backscatter reduce retrieval accuracy. The current measurement dataset is related to continuous measurements conducted between July and August 2020. Each radar was operating in 20-minute measurement cycles consisting of approximately three minutes of passive listening, used to identify a clean frequency band, followed by 17 minutes of active data acquisition. The resulting measurements were averaged to produce three current maps per hour. The analyses presented in this study are based on three-hour averages, corresponding to the mean of nine consecutive 20-minute radial and vector field maps taken to improve accuracy for the flow time-scales of interest. The three-hour average used in the analysis is 12:00-15:00 to coincide with the passage of the satellite over the region.

2.1.4 Cruise Data

N800 cruises — Data were obtained from a pelagic time-series station (N800; 32.52° N, 34.72° E) located 15 km offshore of the Israeli coast at a water depth of 832 m. The results presented here correspond to sampling periods during which coastal filaments were observed to pass over the station (July 2020 and September 2020), together with routine sampling conducted under non-filament conditions for comparison.

Sampling was conducted from the R/V Mediterranean Explorer using a rosette system equipped with 12 Niskin bottles. Hydrographic profiles were obtained with a Sea-Bird Electronics SBE19plusV2 CTD equipped with sensors for conductivity, temperature, fluorescence (used as a proxy for chlorophyll-a; (Zeng and Li, 2015)), turbidity, photosynthetically active radiation (PAR), and, for selected cruises, dissolved oxygen. Sampling was typically conducted between 10:00 and 13:00 local time, coinciding with satellite overpass of the region.

Particulate Fe, Si, and C (and other major element) concentrations were measured using thin-film X-ray fluorescence (XRF) at depths of 20, 100, and 180 m (Paulino et al., 2013). Organic matter (OM) and inorganic matter (IM) were estimated from thin-film XRF measurements of organic carbon and Si. OM was calculated as twice the measured organic carbon concentration, while IM was estimated assuming that Si constitutes 20 % of total inorganic particulate matter (Goldsmith et al., 2001).

Detailed descriptions of the sampling procedures and analytical methods for dissolved nutrients and major particulate elements measured by thin-film XRF are provided in Ben-Ezra et al. (2024).

https://doi.org/10.5194/egusphere-2026-1507
Preprint. Discussion started: 24 March 2026

2.2 Methods

2.2.1 Detection of high-chlorophyll offshore eddies

Satellite-derived chlorophyll fields were used to detect coastal mesoscale eddies characterized by elevated surface chlorophyll relative to the open-sea background. A threshold of twice the mean offshore background chlorophyll concentration—defined as the mean of values between the 20th and 80th percentiles seaward of the 700 m isobath—was applied to each daily map. Because our objective was to quantify coastal waters that are advected offshore, we restricted the analysis to waters deeper than the -700 m isobath. In the Eastern Levantine Basin this depth lies seaward of the continental slope, so any water mass detected beyond this contour can be considered to have left the coastal domain and entered the open-basin environment.

Contiguous regions exceeding the threshold were labeled as individual eddies. The horizontal surface area of each eddy was calculated by converting grid-cell dimensions on the latitude–longitude grid into true spherical cell areas and summing over all cells within the mask.

To quantify the three-dimensional chlorophyll anomaly associated with each eddy, these surface detections were combined with glider-derived vertical profiles. Eddy-period profiles $C_{\mathrm{eddy}}(z)$ were compared with a reference profile $C_{\mathrm{ref}}(z)$ obtained outside the eddy. The vertical anomaly profile was defined as

$$\Delta C(z) = C_{\mathrm{eddy}}(z) - C_{\mathrm{ref}}(z),$$

with both positive and negative contributions retained to allow for the possibility of net depletion as well as enrichment. The vertically integrated anomaly per unit area is

$$I = \int_0^{z_{\max}} \Delta C(z)\, dz,$$

where $z_{\max}$ is the maximum depth over which both the eddy and reference profiles are defined. The total anomaly volume is then

$$V = A_{\mathrm{eddy}}\, I,$$

where A_{eddy} is the horizontal area of the detected eddy.

2.2.2 Gradient-based detection of the eddy frontal boundary

To identify the dynamically active boundary of the coastal mesoscale eddy, we applied a combined gradient–amplitude detection method to daily satellite chlorophyll fields. Horizontal chlorophyll gradients were first computed in metric units to quantify spatial frontal intensity. A robust gradient threshold was then defined from offshore values as the 90th percentile of the gradient magnitude,

$$|\nabla C| \geq G_{\mathrm{thr}}, \qquad G_{\mathrm{thr}} = \mathrm{percentile}_{90}\left(|\nabla C|_{\mathrm{offshore}}\right),$$

https://doi.org/10.5194/egusphere-2026-1507
Preprint. Discussion started: 24 March 2026

thereby isolating regions of anomalously strong horizontal gradients relative to background offshore variability.

To ensure that detected features also corresponded to elevated chlorophyll concentrations, an adaptive amplitude threshold was applied,

$$C \geq C_{\mathrm{amp}}, \qquad C_{\mathrm{amp}} = 1.5 \times \mathrm{percentile}_5(C_{\mathrm{offshore}}),$$

which retains only statistically significant chlorophyll anomalies above the offshore background level.

Pixels satisfying both the gradient and amplitude criteria, and located seaward of the -700 m isobath, were combined to form a preliminary eddy mask. Connected-component labeling was then used to isolate spatially coherent structures, and the largest structure was selected for each day. Its boundary was extracted using isocontour reconstruction to obtain a closed polygon representing the northeastern frontal limb of the coastal mesoscale eddy, corresponding to the leading edge of the eddy as it propagates eastward.

This polygon was used to collocate HF-radar observations. A manually selected eddy center was used to compute the radial direction at each HF measurement point, and azimuthal velocities were obtained by projecting the HF vectors onto the tangential direction. Maximum, minimum, and mean azimuthal speeds were computed from all HF measurements falling within the frontal polygon. This approach isolates the dynamically coherent frontal region of the eddy and enables estimation of both rotational strength and downstream propagation.

3 Results

3.1 Regional context: summertime mesoscale activity and basin-scale biogeochemical structure

A basin-scale snapshot of summer surface conditions in the Eastern Mediterranean Sea (30 July 2020) reveals a close correspondence between mesoscale circulation and surface chlorophyll distributions (Fig. 1). Offshore regions characterized by anticyclonic circulation and elevated sea surface height (SSH), for example, the Shikmona Gyre and Cyprus Eddy (Zodiatis et al., 2023; Bergamasco and Malanotte-Rizzoli, 2010; Robinson and Golnaraghi, 1994), are associated with uniformly low chlorophyll concentrations, consistent with strong stratification and suppressed nutrient supply (Belkin et al., 2022). In contrast, cyclonic features identified by depressed SSH, such as the Rhodes Gyre (van Leeuwen et al., 2022), coincide with locally enhanced surface chlorophyll, reflecting their upwelling-favorable dynamical setting.

Along the southern Levantine coast, surface chlorophyll concentrations are not uniformly elevated relative to the offshore basin. Instead, enhanced coastal chlorophyll is primarily observed downstream of the Nile River Delta, the dominant source of nutrient-rich coastal waters in the region (Nixon, 2003; El-Rayis and Abdallah, 2006; Oczkowski et al., 2009). This downstream asymmetry is evident in the distribution of coastal mesoscale features: anticyclonic eddies located west of the Nile Delta (upstream) exhibit little to no surface chlorophyll enhancement (Fig. 1A,C - 31.5° N, 28.75° E), whereas anticyclonic eddies and filamentary structures east of the Delta (downstream) display pronounced surface chlorophyll signatures (Fig. 1A),(Fadida et al., 2026).

https://doi.org/10.5194/egusphere-2026-1507
Preprint. Discussion started: 24 March 2026

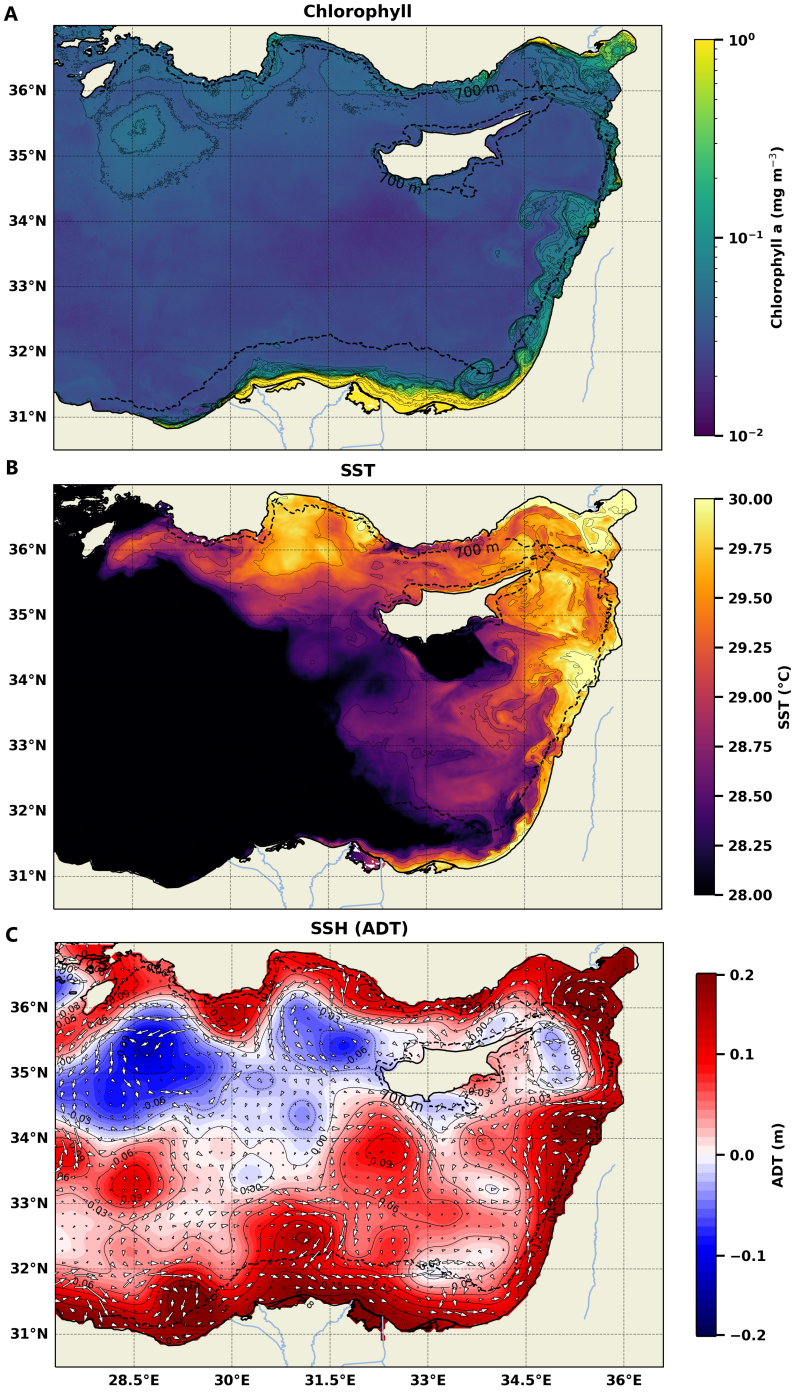

Figure 1. Summer surface conditions in the Eastern Levantine Basin on 30 July 2020. A. Surface chlorophyll (mg m^{-3}), highlighting a sequence of mesoscale eddies extending downstream of the Nile River Delta and progressing cyclonically across the basin. The 700 m isobath is shown as a black dotted line. B. Sea surface temperature (SST) and C. Absolute dynamic topography (ADT) with geostrophic currents.

https://doi.org/10.5194/egusphere-2026-1507
Preprint. Discussion started: 24 March 2026

Against this basin-wide background, during summer, a sequence of mesoscale meanders and eddies is embedded in the Levantine along-shore coastal current (Fig. 1A-C). Unlike the offshore anticyclonic features, these downstream coastal eddies exhibit elevated surface chlorophyll concentrations despite their anticyclonic nature. The associated sea surface temperature field (Fig. 1B) further indicates that these features are composed of relatively warm coastal-origin waters that are advected along the shoreline.

The regional snapshot further shows that coastal mesoscale features are dynamically connected to the larger-scale circulation. In particular, one of the downstream coastal eddies is observed to extend offshore and merge with the Shikmona Gyre (33.41° N, 34.25° E), suggesting a direct pathway by which Nile-influenced coastal waters can be transferred into the open sea. This basin-scale context highlights coastal eddies and filaments as a distinct class of mesoscale features whose biogeochemical signature reflects both their dynamical structure and their upstream conditioning within the coastal boundary current.

3.2 Eddy coherence, kinematics, and propagation

To determine whether the downstream coastal features identified in Fig. 1 represent dynamically coherent mesoscale eddies rather than transient surface tracer patches, we analyzed a series of collocated satellite chlorophyll imagery and HF-radar surface current measurements from 30 July to 3 August 2020 (Fig. 2). Over five consecutive days, satellite observations captured the downstream evolution of a coastal anticyclonic feature, whose leading northeastern frontal segment advanced seaward along the Levantine coast.

Tracking the displacement of this frontal boundary indicates that the eddy propagated at a mean speed of approximately 0.155 m s^{-1} ($\sim$13.4 km day^{-1}). Concurrent HF-radar measurements reveal a well-defined azimuthal circulation that is spatially collocated with the chlorophyll-defined eddy boundary. Maximum tangential velocities ranged from 0.11–0.36 m s^{-1} on 30 July, 0.30–0.64 m s^{-1} on 31 July, and 0.37–0.73 m s^{-1} on 1 August, 0.14–0.93 m s^{-1} on 2 August, and 0.05–0.67 m s^{-1} on 3 August, with mean values ranging from 0.21 to 0.68 m s^{-1} over the same period.

At all stages, the measured azimuthal velocities exceeded the downstream propagation speed by a factor of two to six, indicating that the feature was dominated by rotational motion rather than simple advection by the background flow. The persistence of a closed anticyclonic circulation over multiple days confirms that the observed structure represents a dynamically coherent mesoscale eddy.

3.3 Three-dimensional structure of the eddies

To characterize the three-dimensional structure of coastal mesoscale eddies during summer stratification, we analysed two independent autonomous glider missions that intersected coastal eddies identified in satellite imagery. These observations allow direct comparison between the vertical structure within the eddy interior and the surrounding offshore waters.

The first glider mission, conducted during June–July 2018, sampled a coastal eddy over a period of approximately 12 days (Fig. 3). Within the eddy interior, chlorophyll concentrations were elevated throughout the upper water column, and the DCM markedly shoaled, from depths of approximately 120–130 m in ambient offshore waters to about 50 m inside the eddy. Potential density contours exhibited downward displacement within the eddy, consistent with anticyclonic structure and indicating the

https://doi.org/10.5194/egusphere-2026-1507
Preprint. Discussion started: 24 March 2026

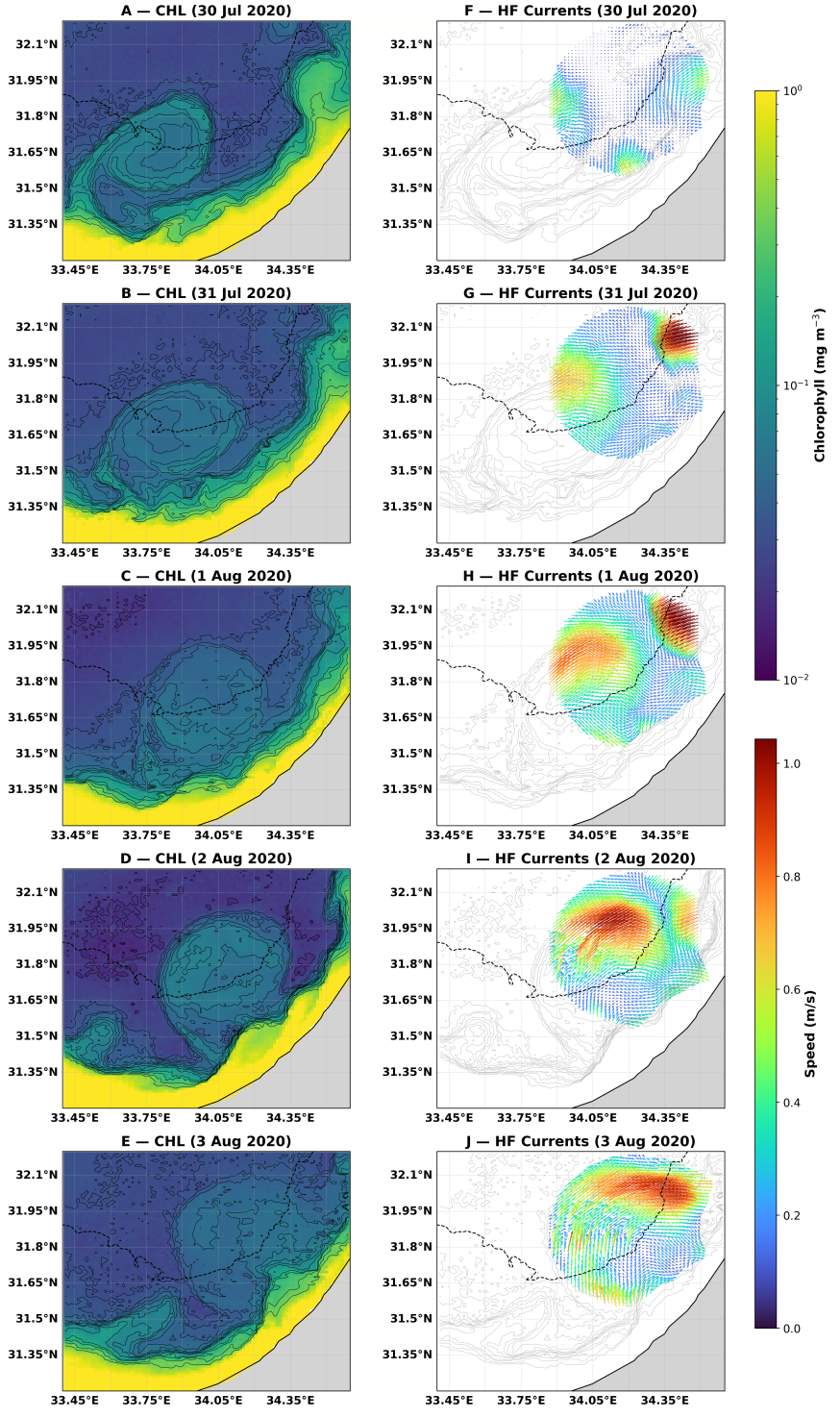

Figure 2. Satellite and HF-radar observations during 30 July–3 August 2020. (A–E) Daily surface chlorophyll maps. (F–J) HF-radar surface currents overlaid on CHL contours.

https://doi.org/10.5194/egusphere-2026-1507
Preprint. Discussion started: 24 March 2026

absence of local upwelling. Sea surface and subsurface temperatures within the eddy were slightly higher than in surrounding offshore waters, consistent with the advection of coastal-origin water masses.

Taken together, these observations show that the 2018 eddy was associated with a coherent reorganization of the hydrographic structure and vertical chlorophyll distribution, characterized by elevated surface concentrations and a shallow DCM despite downwelling-favorable dynamics.

A second glider mission intersected a coastal eddy off of northern Israel in late June 2022 (Fig. 4). Although this mission did not include in situ measurements of temperature or density due to a CTD malfunction, chlorophyll profiles nonetheless revealed a similarly shoaled DCM within the eddy interior relative to adjacent offshore waters. The repetition of this vertical chlorophyll structure in an independent eddy supports the generality of the observed three-dimensional response.

To quantify the offshore influence of coastal eddies, vertical chlorophyll anomaly profiles were computed by subtracting reference profiles sampled outside the eddy from profiles collected within the eddy interior (Figs. 5, 6). These anomaly profiles were vertically integrated and combined with the offshore surface area of each eddy to estimate the excess chlorophyll stock associated with offshore transport.

For the 2018 eddy, the vertically integrated chlorophyll anomaly was positive, reflecting both elevated surface concentrations and a spatially extensive shoaled DCM. The offshore portion of the eddy extended over an area of approximately 1430 km^2, yielding an estimated excess chlorophyll stock of approximately 1500 kg transported offshore.

A similar analysis was performed for the 2022 eddy. Despite differences in eddy size and sampling geometry, the vertically integrated anomaly was again positive. Over a combined offshore surface area of approximately 980 km^2, this corresponded to an estimated excess chlorophyll stock of approximately 3500 kg.

The vertical structure of the anomaly exhibited two contrasting layers in both glider missions: a positive anomaly extending from the surface to approximately 100 m, and a negative anomaly below this depth. The negative anomaly reached its maximum near approximately 100 m in the 2018 eddy and approximately 130 m in the 2022 eddy, indicating a redistribution of chlorophyll within the water column rather than a uniform increase at all depths.

Despite the presence of a pronounced negative anomaly at depth, the vertically integrated anomaly remained positive in both cases. These estimates therefore indicate that coastal mesoscale eddies can produce a net positive offshore chlorophyll anomaly during summer stratification, with event-scale export magnitudes that vary depending on eddy characteristics.

3.4 Biogeochemical footprint of the eddies

Ship-based observations at a fixed offshore location provide independent evidence of coastal water-mass influence, as reflected in the in situ biogeochemical properties. Station N800, located near the continental slope, was sampled approximately monthly throughout 2020, enabling comparison between background summer conditions (June and August) and two sampling periods influenced by coastal mesoscale eddies (July and September).

Satellite-derived surface chlorophyll imagery indicates that the July and September sampling periods coincided with times when station N800 was located within or immediately adjacent to coastal mesoscale eddies propagating offshore (Fig. 7A–B), whereas the June and August profiles were collected under background conditions without direct eddy influence.

https://doi.org/10.5194/egusphere-2026-1507
Preprint. Discussion started: 24 March 2026

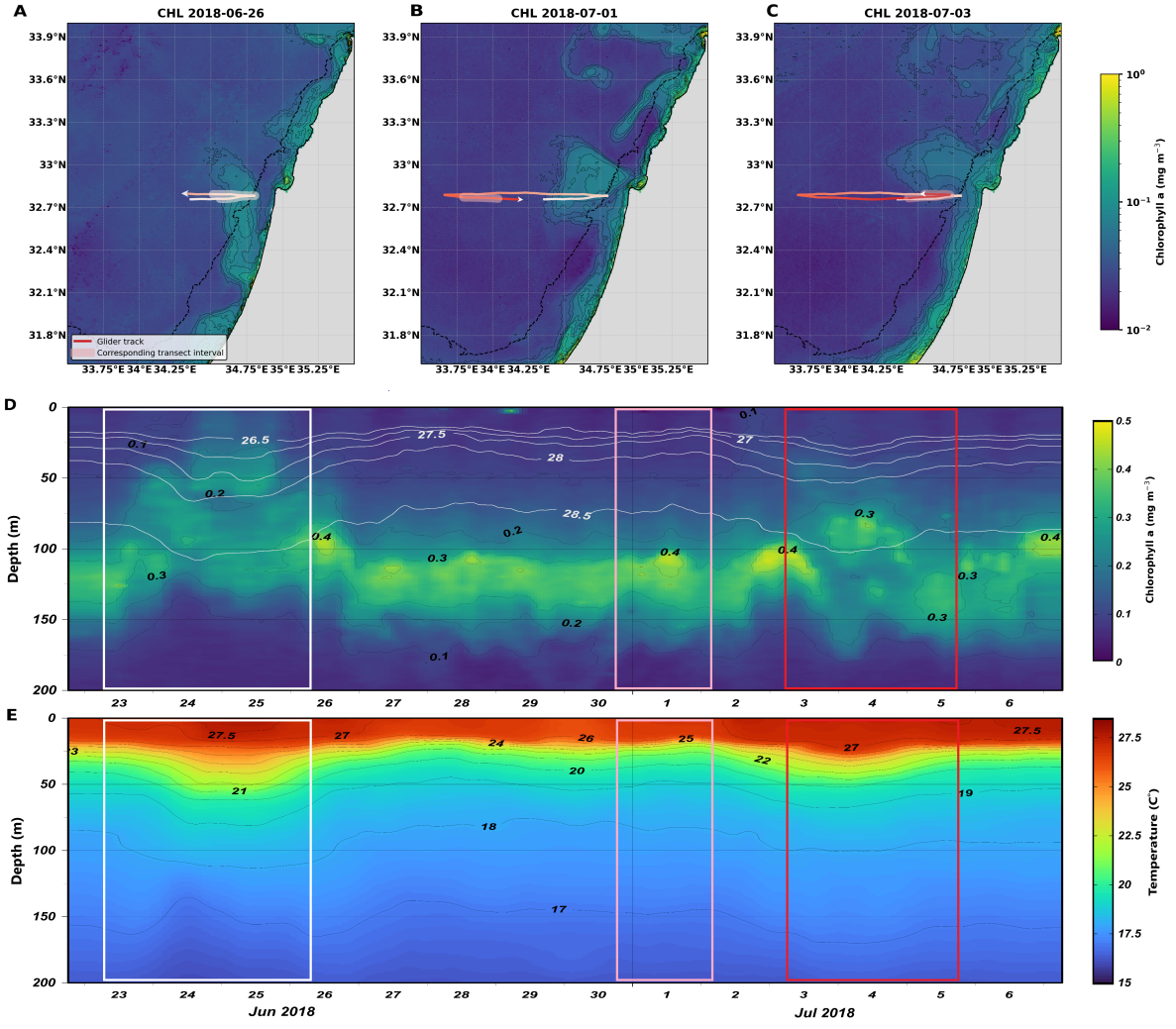

Figure 3. Satellite and glider observations of a coastal eddy during June/July 2018. (A–C) Surface chlorophyll on 26 June, 1 July, and 3 July, with the cumulative glider trajectory colored by time progression. Lightened segments mark the position of the glider at the time of each satellite image. (D) Glider-derived chlorophyll section (mg m^{-3}), with density anomaly contours (white). Colored rectangles indicate the portions of the transect corresponding to the satellite snapshots, using the same color progression as in (A–C). (E) Glider-derived temperature section (C°), with the same highlighted intervals as in (D).

https://doi.org/10.5194/egusphere-2026-1507
Preprint. Discussion started: 24 March 2026

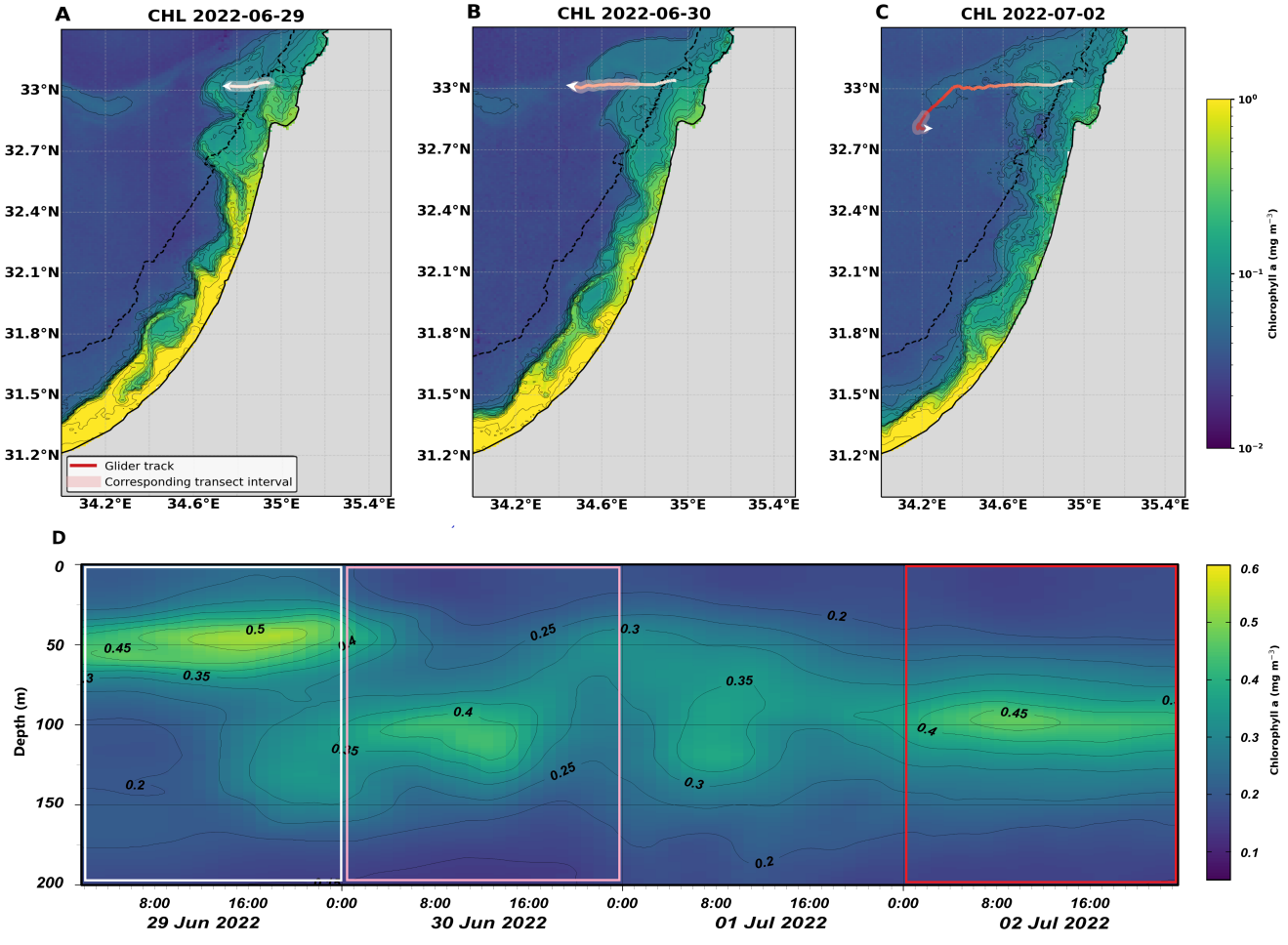

Figure 4. Satellite and glider observations of a coastal eddy during June–July 2022. (A–C) Daily surface chlorophyll with the cumulative glider trajectory overlaid and colored by time progression. Lightened segments mark the position of the glider at the time of each satellite image. (D) Glider-derived chlorophyll section (mg m^{-3}), with colored rectangles indicating the corresponding portions of the transect, using the same color progression as in (A–C).

https://doi.org/10.5194/egusphere-2026-1507
Preprint. Discussion started: 24 March 2026

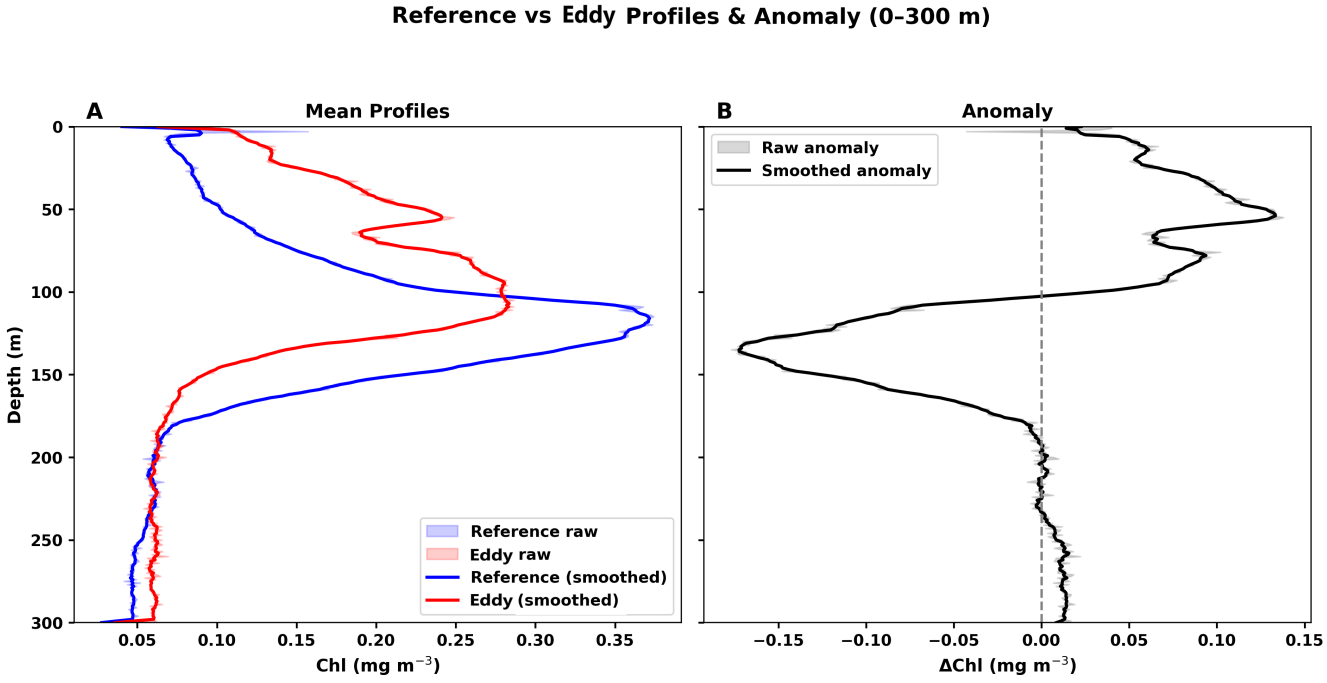

Figure 5. A. Depth profiles of chlorophyll during the reference period (28–29 June 2018; blue) and the eddy period (24–26 June 2018; red). (B) Chlorophyll anomaly profile (eddy minus reference; black).Shaded and solid lines denote raw and smoothed profiles, respectively.

At N800, dissolved silica concentrations in the upper water column were higher in July and September 2020 than in the other summer months (Fig. 7C). In July, the increase was largely confined to the surface layer, whereas in September elevated concentrations extended to 50 m depth. These changes coincided with enhanced particulate inputs (Fig. 7D). Total inorganic particulate matter, calculated from measurements at 25, 100, and 180 m, was substantially higher in July and September than in the other months. Particulate Fe concentrations (Fig. 7E) were also elevated, extending through the upper 100 m in July and the upper 180 m in September.

Concurrent with these changes in dissolved and particulate constituents, the vertical chlorophyll structure (Fig. 7F) differed from typical summer conditions. Profiles from June and August exhibited the characteristic offshore Levantine summer pattern, with a pronounced deep chlorophyll maximum (DCM) at 120–130 m. In contrast, the July and September profiles showed a broadened chlorophyll distribution and a reorganization of the vertical structure, including enhanced concentrations higher in the water column. While the increase remained associated with the top of the nutricline, as in background conditions, chlorophyll concentrations were elevated over a thicker depth range extending upward to 50 m in July and 35 m in September, resulting in a shoaled and, in some cases, bimodal DCM.

Together, these observations show that at a fixed offshore location, the passage of coastal mesoscale eddies is associated with higher dissolved nutrient concentrations and increased inorganic particulate matter (including particulate Fe, but not total

https://doi.org/10.5194/egusphere-2026-1507
Preprint. Discussion started: 24 March 2026

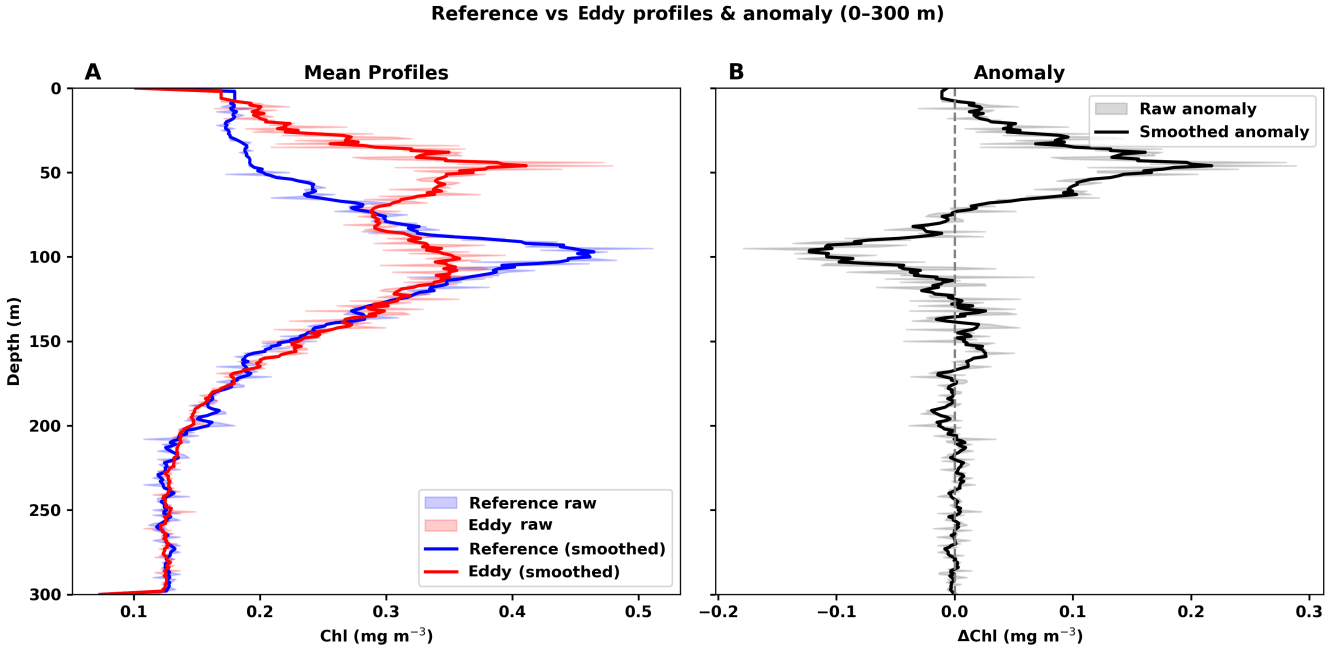

Figure 6. Depth profiles of chlorophyll during the reference period (2–3 July 2022; blue) and eddy period (29 June 2022; red). (A) Raw and smoothed profiles. (B) Chlorophyll anomaly profile (eddy minus reference).

organic matter), accompanied by a broadening and upward redistribution of chlorophyll relative to typical stratified summer conditions.

4 Discussion

4.1 Summertime connectivity and the role of coastal mesoscale eddies

265 During summer stratification, the Eastern Mediterranean Sea is generally characterized by weak coastal–offshore connectivity. Strong vertical stratification suppresses nutrient resupply to the surface, while the persistent alongshore boundary current limits cross-shore exchange, effectively isolating the offshore Levantine Basin from coastal influences (Estrada, 1996; Rosentraub and Brenner, 2007; Ozer et al., 2022). Under these conditions, lateral transport of coastal waters into the open sea is generally expected to be minimal.

270 The results presented here identify coastal mesoscale eddies as intermittent features that can locally disrupt this summer isolation. These eddies form along the coastal boundary current and propagate downstream while maintaining a dynamically coherent internal circulation, as evidenced by HF-radar observations showing rotational velocities that substantially exceed their translational speed (Chelton et al., 2011; McWilliams, 1985). Similar mesoscale features have been documented along the Levantine coast in observations and models (Menna et al., 2012; Efrati et al., 2013; Estournel et al., 2021; Baaklini et al.,

https://doi.org/10.5194/egusphere-2026-1507
Preprint. Discussion started: 24 March 2026

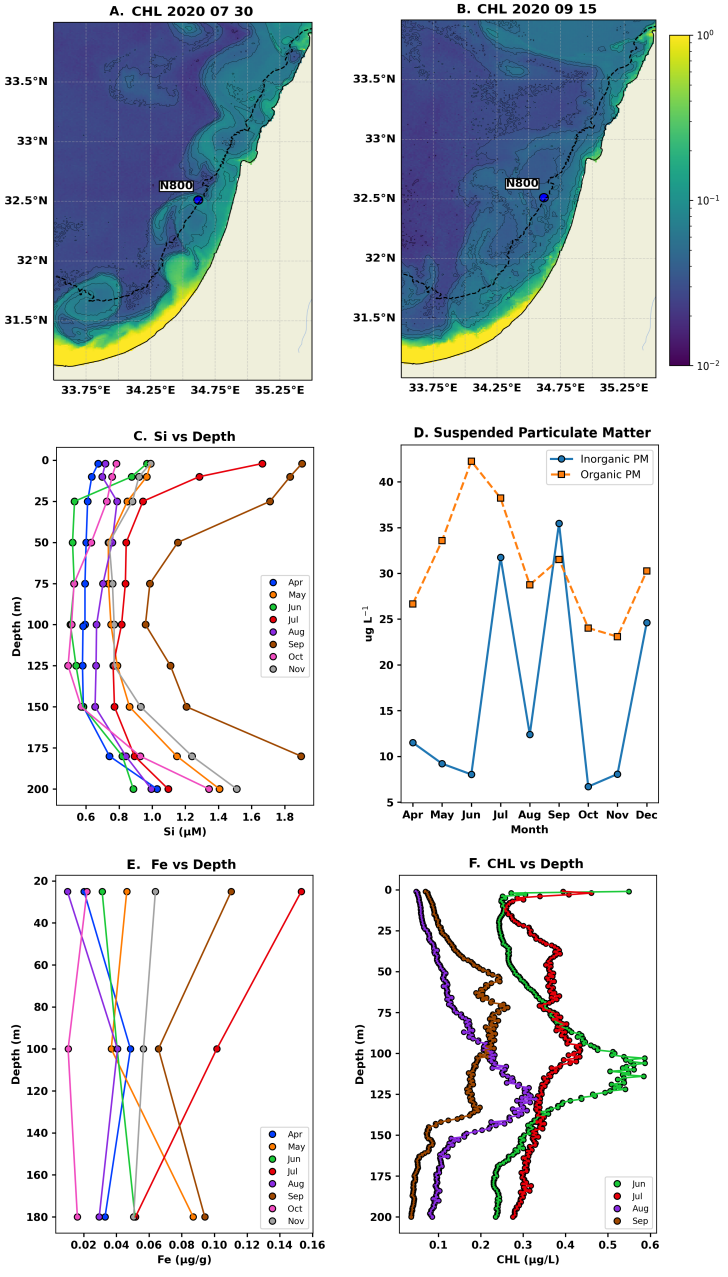

Figure 7. Monthly variability in dissolved and particulate properties at time-series station N800. (A–B) Satellite-derived surface chlorophyll fields corresponding to the anomalous sampling dates. (C) Vertical profiles of dissolved silicic acid Si(OH)4 (μM). (D) Monthly integrated suspended particulate matter. (E) Vertical profiles of particulate Fe (μg g^{-1}). (F) Vertical profiles of chlorophyll fluorescence (μg L^{-1}).

https://doi.org/10.5194/egusphere-2026-1507
Preprint. Discussion started: 24 March 2026

2024), and satellite data indicate that they recur during summer (Akpınar, 2024; Verma et al., 2024). Their episodic nature implies that coastal–offshore exchange during the stratified season is not sustained but instead occurs through discrete events. Taken together, these results indicate that coastal mesoscale eddies act as intermittent pathways for cross-shore exchange during summer stratification in the Eastern Mediterranean, intermittently extending offshore and exporting vertically structured coastal water masses into an otherwise weakly productive environment. This mechanism complements wintertime mixing and submesoscale stirring (Lévy et al., 2012), highlighting the role of mesoscale dynamics in shaping seasonal connectivity in ultra-oligotrophic systems.

4.2 Vertical structure and coastal water-mass signatures

The influence of coastal mesoscale eddies extends beyond surface tracer redistribution and involves a consistent reorganization of the upper water column. Glider observations demonstrate that eddy interiors are characterized by elevated chlorophyll concentrations and a pronounced shoaling and broadening of the DCM relative to background offshore conditions. Such a shallow DCM contrasts with the deep, well-defined offshore DCM typically observed during summer stratification in the Levantine Basin (Mignot et al., 2014; Teruzzi et al., 2021; Ediger and Yilmaz, 1996; Ben-Ezra et al., 2024).

The vertical structure of these features provides insight into their underlying dynamics and origin. In the primary glider case (Fig. 3), the broadened and shoaled DCM occurs in conjunction with downward-displaced density surfaces, consistent with anticyclonic, downwelling-favorable circulation. This combination rules out local upwelling as the driver of enhanced upper-layer chlorophyll and instead indicates lateral advection of a preconditioned coastal water mass into the offshore environment, a mechanism also reported in other stratified boundary current systems (Cornec et al., 2021; Espinosa-Carreón et al., 2012; Xu et al., 2023). Elevated surface and subsurface temperatures observed within the eddy further support this interpretation.

Independent ship-based observations at the time-series station N800 further support these findings. Periods influenced by coastal mesoscale eddies were characterized by elevated Silicate concentrations in the upper water column, increased amounts of fine-grained inorganic particles, and a modified vertical chlorophyll structure. Consistent with this interpretation, CTD observations at station N800 show lower surface salinity and higher surface temperature during the July eddy (Fig. A1A,B), indicative of coastal-origin water previously described for the southeastern Levantine Basin (Ozer et al., 2022). Rather than exhibiting the typical, well-defined deep chlorophyll maximum (DCM), chlorophyll began increasing at the top of the nutricline, as under normal conditions, but the distribution was broadened and intensified upward, extending to depths of approximately 35–50 m. A plausible mechanism is that, as the coastal eddy forms, its current is sufficiently strong to resuspend the uppermost sediments of the adjacent shelf, which includes fine-grained sediment. This resuspended layer contains benthic phytoplankton (Rubin-Blum et al., 2022) and is likely enriched in nutrients due to in situ heterotrophic bacterial activity. Consequently, the eddy core is transported from the shelf into pelagic waters, carrying elevated dissolved and particulate nutrient concentrations (Fig. 7). The dissolved nutrients introduced to pelagic waters have the capacity to stimulate new primary production which, combined with sinking particles with benthic phytoplankton attached, contribute to the observed enhanced chlorophyll signal. Vertical chlorophyll structure at station N800 closely resembled that observed during the glider missions. Although anomaly profiles were not explicitly calculated for the N800 data, the vertical distributions during eddy-influenced months showed

https://doi.org/10.5194/egusphere-2026-1507
Preprint. Discussion started: 24 March 2026

enhanced chlorophyll in the upper 100 m and comparatively reduced concentrations at greater depths, consistent with the two-layer anomaly structure identified from the glider analysis. PAR profiles from the N800 cruises (Fig. A1C) further showed a divergence beginning near 40 m, with lower subsurface PAR during the July and September eddy periods relative to the June and August reference profiles. This reduction in light penetration provides a plausible mechanism for the observed deep chlorophyll suppression. The elevated chlorophyll concentrations and increased suspended particulate matter associated with eddy influence likely enhanced light attenuation in the upper water column, further reducing subsurface PAR and contributing to the negative anomaly at depth, consistent with established relationships between particle concentrations, optical attenuation, and underwater light availability (Babin et al., 2003; Neukermans et al., 2014; Morel and Maritorena, 2001). Coastal waters in the Eastern Mediterranean receive terrestrial and benthic nutrient inputs; however, anti-estuarine circulation and rapid biological uptake limit the accumulation of nutrients and prevent the development of a persistent cross-shore nutrient gradient (Kress and Herut, 1998; Ben-Ezra et al., 2023; Krom et al., 2010). Consequently, coastal biogeochemical signals are often short-lived or spatially heterogeneous, and may only become clearly expressed offshore when transported within mesoscale features (Efrati et al., 2013). The recurrence of these vertical signatures across various sampling strategies suggests that the observed reorganization reflects a persistent property of the advected water mass rather than transient biological responses to local forcing.

4.3 Event-scale offshore redistribution under stratified conditions

The vertical reorganization associated with coastal mesoscale eddies results in a measurable redistribution of chlorophyll within the offshore water column. By combining vertically integrated chlorophyll anomaly profiles with the offshore surface area of individual eddies, the results provide event-scale estimates of the excess chlorophyll transported offshore during summer stratification (1500-3500 kg per eddy). Similar event-based approaches have been used to assess eddy-driven transport in other oligotrophic systems (Gerin et al., 2009; Martin, 2003). For both glider-sampled eddies, the vertically integrated chlorophyll anomaly was positive, reflecting the combined effects of elevated surface concentrations and a shoaled DCM relative to background offshore conditions. Although the absolute magnitudes differed between events, the consistent sign of the anomaly indicates that coastal mesoscale eddies can act as net exporters of chlorophyll and nutrients into the offshore Levantine Basin during summer.

In an ultra-oligotrophic system such as the eastern Levantine Basin (Krom et al., 2005; Herut et al., 2000), even modest event-scale anomalies may be biogeochemically relevant. Background offshore chlorophyll concentrations are extremely low, and phytoplankton biomass during summer is largely confined to a narrow depth range near the nutricline (Mignot et al., 2014; Teruzzi et al., 2021). The episodic introduction of coastal-origin biomass into the upper offshore water column therefore represents a perturbation to an otherwise weakly productive system. Because eddy occurrence is episodic and interception by in situ platforms is limited, these estimates cannot be robustly extrapolated to seasonal or basin-wide budgets and should be interpreted as first-order, event-scale indicators of offshore redistribution.

https://doi.org/10.5194/egusphere-2026-1507
Preprint. Discussion started: 24 March 2026

4.4 Broader context and limitations

Coastal eddies and filaments have been shown to facilitate cross-shelf exchange in a range of boundary current systems, often transporting nutrient rich waters offshore and enhancing biological productivity (Flos and Tintoré, 1990; Espinosa-Carreón et al., 2012; Wang et al., 2018). In many of these regions, however, coastal–offshore contrasts in nutrients and biomass are substantially larger than in the Eastern Mediterranean, and background productivity is higher.

The Levantine Basin represents a limiting case, where nutrient concentrations and surface chlorophyll are among the lowest observed globally (Krom et al., 2005; Pujo-Pay et al., 2011). In this context, the presence of detectable biogeochemical signatures associated with coastal eddies highlights that even modest coastal enrichment can be preserved and transported offshore when embedded within dynamically coherent mesoscale structures. The Eastern Mediterranean therefore provides a useful natural laboratory for examining eddy-driven exchange under ultra-oligotrophic conditions.

The conclusions drawn here are subject to several observational limitations. Interception of coastal mesoscale eddies by autonomous gliders and ship-based sampling is inherently opportunistic and constrained by platform trajectories and sampling schedules. In addition, the export estimates rely on assumptions regarding eddy geometry, representativeness of vertical profiles, and the choice of background reference conditions. While these assumptions are physically motivated and internally consistent, they introduce uncertainty that limits quantitative extrapolation beyond the sampled events.

5 Conclusions

Coastal mesoscale eddies provide an intermittent but effective pathway for cross-shore exchange during summer stratification in the Eastern Mediterranean, exporting coastal water into the otherwise isolated offshore Levantine Basin. Although these features are predominantly anticyclonic and typically associated with downwelling and low productivity in pelagic regions, their formation in proximity to the coast allows them to entrain relatively enriched waters. As a result, they transport elevated chlorophyll, nutrients, and suspended particulate matter offshore, along with a distinct vertical structure characterized by a shallow, often bimodal DCM.

These findings highlight how mesoscale dynamics can modify the expected biogeochemical role of anticyclonic eddies and emphasize their importance as episodic drivers of offshore redistribution in ultra-oligotrophic environments.

Data availability. This study has been conducted using E.U. Copernicus Marine Service;
DOI: 10.48670/moi-00300 (product name: $OCEANCOLOUR\_MED\_BGC\_L4\_MY$).
DOI: 10.48670/moi-00142 (product name: $SEALEVEL\_EUR\_PHY\_L4\_NRT\_008\_060$).
DOI: 10.48670/moi-00172 (product name: $SST\_MED\_SST\_L4\_NRT\_OBSERVATIONS\_010\_004\_c\_V2$).

https://doi.org/10.5194/egusphere-2026-1507
Preprint. Discussion started: 24 March 2026

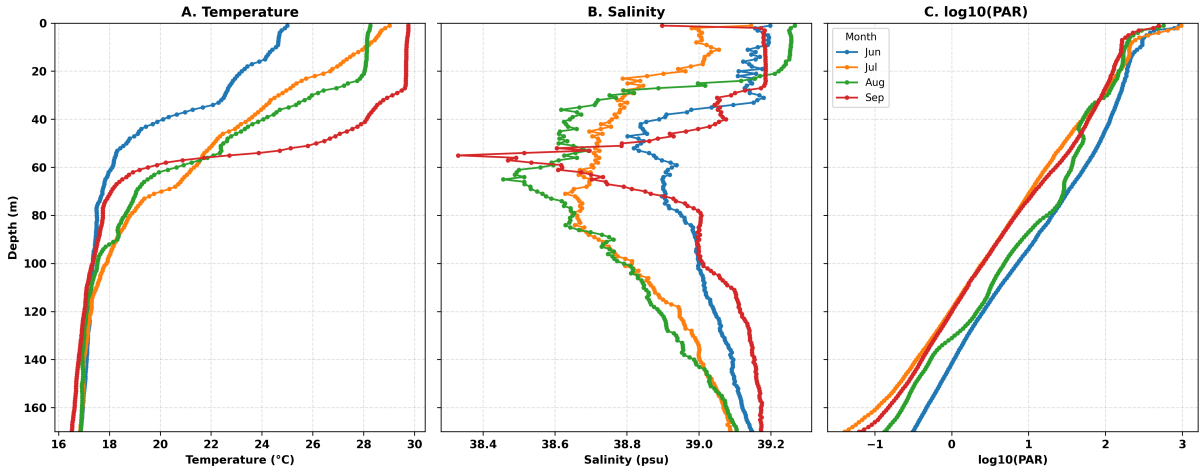

Figure A1. Vertical profiles of A. **temperature**, B. **salinity**, and C. $\log_{10}(\mathrm{PAR})$ at station N800 during June–September 2020. Profiles are derived from individual ship-based measurements and shown from the surface to 170 m depth. Photosynthetically active radiation (PAR) was recalculated from measured values using a 3 m depth-smoothed moving average prior to log-transformation.

Appendix A

Author contributions. Y.F. compiled, processed, and analyzed the satellite and glider data. T.O. collected and processed the glider data. T.BE., M.D.K., A.T., and M.T. collected, processed, analysed, and interpreted the cruise data. Y.T. collected and processed the HF radar data. Y.L. and E.B. oversaw the research. Y.F., Y.L, M.D.K., T.O., T.BE. and E.B. interpreted the results. Y.F. led the writing of the paper with contributions from all coauthors.

Competing interests. The authors declare they have no competing interests.

Acknowledgements. This research has been supported by the Israel Science Foundation (grant nos. 1266/23). The glider mission M141 was financed by the Italian Ministry of Foreign Affairs and the Israeli Ministry of Innovation, Science and Technology (as part of the MELMAS project. The cruise data in this study were made possible by the MKMRS monitoring cruise series, as well as the Charney School of Marine Sciences, with support by the captain and crew of the MedExplorer and EcoOcean. The authors acknowledge the use of ChatGPT (OpenAI) for assistance with language editing and phrasing of parts of the manuscript. All scientific content, interpretations, and conclusions are solely those of the authors.

https://doi.org/10.5194/egusphere-2026-1507
Preprint. Discussion started: 24 March 2026

References

Akpınar, A.: Seasonal and Interannual Variability in Sea Surface Temperature Fronts in the Levantine Basin, Mediterranean Sea, Journal of Marine Science and Engineering, 12, https://doi.org/10.3390/jmse12081249, 2024.

Alkalay, R., Zlatkin, O., Katz, T., Herut, B., Halicz, L., Berman-Frank, I., and Weinstein, Y.: Carbon export and drivers in the southeastern Levantine Basin, Deep Sea Research Part II: Topical Studies in Oceanography, 171, 104 713, https://doi.org/https://doi.org/10.1016/j.dsr2.2019.104713, revisiting the Eastern Mediterranean: Recent knowledge on the physical, biogeochemical and ecosystemic states and trends (Volume II), 2020.

Azov, Y.: Seasonal patterns of phytoplankton productivity and abundance in nearshore oligotrophic waters of the Levant Basin (Mediterranean), Journal of Plankton Research, 8, 41–53, https://doi.org/10.1093/plankt/8.1.41, 1986.

Baaklini, G., Brajard, J., Issa, L., Fifani, G., Mortier, L., and El Hourany, R.: Monitoring the coastal–offshore water interactions in the Levantine Sea using ocean color and deep supervised learning, Ocean Science, 20, 1707–1720, https://doi.org/10.5194/os-20-1707-2024, 2024.

Babin, M., Stramski, D., Ferrari, G. M., Claustre, H., Bricaud, A., Obolensky, G., and Hoepffner, N.: Variations in the light absorption coefficients of phytoplankton, nonalgal particles, and dissolved organic matter in coastal waters around Europe, Journal of Geophysical Research: Oceans, 108, https://doi.org/https://doi.org/10.1029/2001JC000882, 2003.

Barale, V., Jaquet, J.-M., and Ndiaye, M.: Algal blooming patterns and anomalies in the Mediterranean Sea as derived from the SeaWiFS data set (1998–2003), Remote Sensing of Environment, 112, 3300–3313, https://doi.org/https://doi.org/10.1016/j.rse.2007.10.014, earth Observations for Marine and Coastal Biodiversity and Ecosystems Special Issue, 2008.

Barrick, D. E.: Extraction of wave parameters from measured HF radar sea-echo Doppler spectra, Radio Science, 12, 415–424, https://doi.org/https://doi.org/10.1029/RS012i003p00415, 1977.

Belkin, N., Guy-Haim, T., Rubin-Blum, M., Lazar, A., Sisma-Ventura, G., Kiko, R., Morov, A. R., Ozer, T., Gertman, I., Herut, B., and Rahav, E.: Influence of cyclonic and anticyclonic eddies on plankton in the southeastern Mediterranean Sea during late summertime, Ocean Science, 18, 693–715, https://doi.org/10.5194/os-18-693-2022, 2022.

Ben-Ezra, T., Reich, T., Tsemel, A., Berman-Frank, I., Lehahn, Y., Sher, D., Suari, Y., and Krom, M.: Nutrient dynamics across the Israeli coastal shelf: An unusual oligotrophic coastal system, Continental Shelf Research, 266, 105 103, https://doi.org/10.1016/j.csr.2023.105103, 2023.

Ben-Ezra, T., Blachinsky, A., Gozali, S., Tsemel, A., Fadida, Y., Tchernov, D., Lehahn, Y., Tsagaraki, T. M., Berman-Frank, I., and Krom, M.: Interannual changes in nutrient and phytoplankton dynamics in the Eastern Mediterranean Sea (EMS) predict the consequences of climate change; results from the Sdot-Yam Time-series station 2018-2022, bioRxiv, https://doi.org/10.1101/2024.06.24.600321, 2024.

Bergamasco, A. and Malanotte-Rizzoli, P.: The circulation of the Mediterranean Sea: a historical review of experimental investigations, Advances in Oceanography and Limnology, 1, 11–28, https://doi.org/10.1080/19475721.2010.491656, 2010.

Berman, T., Townsend, D., Elsayed, S., Trees, C., and Azov, Y.: Optical transparency, chlorophyll and primary productivity in the eastern mediterranean near the israeli coast, Oceanologica Acta, 7, 367–372, https://archimer.ifremer.fr/doc/00131/24219/, 1984.

Berthon, J.-F. and Zibordi, G.: Bio-optical relationships for the northern Adriatic Sea, International Journal of Remote Sensing - INT J REMOTE SENS, 25, 1527–1532, https://doi.org/10.1080/01431160310001592544, 2004.

Chelton, D. B., Schlax, M. G., and Samelson, R. M.: Global observations of nonlinear mesoscale eddies, Progress in Oceanography, 91, 167–216, https://doi.org/https://doi.org/10.1016/j.pocean.2011.01.002, 2011.

https://doi.org/10.5194/egusphere-2026-1507
Preprint. Discussion started: 24 March 2026

Cornec, M., Laxenaire, R., Speich, S., and Claustre, H.: Impact of Mesoscale Eddies on Deep Chlorophyll Maxima, Geophysical Research Letters, 48, e2021GL093 470, https://doi.org/https://doi.org/10.1029/2021GL093470, e2021GL093470 2021GL093470, 2021.

Crombet, Y., Leblanc, K., Quéguiner, B., Moutin, T., Rimmelin, P., Ras, J., Claustre, H., Leblond, N., Oriol, L., and Pujo-Pay, M.: Deep silicon maxima in the stratified oligotrophic Mediterranean Sea, Biogeosciences, 8, 459–475, https://doi.org/10.5194/bg-8-459-2011, 2011.

Crombie, D. D.: Doppler Spectrum of Sea Echo at 13.56 Mc./s., Nature, 175, 681–682, https://doi.org/10.1038/175681a0, 1955.

Ediger, D. and Yilmaz, A.: Characteristics of deep chlorphyll maximum in the Northeastern Mediterranean with respect to environmental conditions, Journal of Marine Systems, 9, 291–303, https://doi.org/https://doi.org/10.1016/S0924-7963(96)00044-9, 1996.

Efrati, S., Lehahn, Y., Rahav, E., Kress, N., Herut, B., Gertman, I., Goldman, R., Ozer, T., Lazar, M., and Heifetz, E.: Intrusion of coastal waters into the pelagic eastern Mediterranean: in situ and satellite-based characterization, Biogeosciences, 10, 3349–3357, https://doi.org/10.5194/bg-10-3349-2013, 2013.

El-Rayis, O. and Abdallah, M.: Contribution of Nutrients and some Trace Metals from a Huge Egyptian Drain to the SE-Mediterranean Sea, west of Alexandria, Mediterranean Marine Science, 7, 79–86, https://doi.org/10.12681/mms.179, 2006.

Espinosa-Carreón, T. L., Gaxiola-Castro, G., Beier, E. J., Strub, P. T., and Kurczyn, J. A.: Effects of mesoscale processes on phytoplankton chlorophyll off Baja California, Journal of Geophysical Research, 117, https://api.semanticscholar.org/CorpusID:129296456, 2012.

Estournel, C., Marsaleix, P., and Ulses, C.: A new assessment of the circulation of Atlantic and Intermediate Waters in the Eastern Mediterranean, Progress in Oceanography, 198, 102 673, https://doi.org/10.1016/j.pocean.2021.102673, 2021.

Estrada, M.: Primary production in the northwestern Mediterranean, 1996.

Fadida, Y., Verma, V., Barkan, R., Biton, E., Solodoch, A., and Lehahn, Y.: Coastal-to-offshore submesoscale horizontal stirring enhances wintertime phytoplankton blooms in the ultra-oligotrophic Eastern Mediterranean Sea, Ocean Science, 22, 329–343, https://doi.org/10.5194/os-22-329-2026, 2026.

Flos, J. and Tintoré, J.: Summer frontal contribution to the fertilization of oceanic waters off the northeast coast of Spain, 1990.

Gerin, R., Poulain, P.-M., Taupier-Letage, I., Millot, C., Ben Ismail, S., and Sammari, C.: Surface circulation in the Eastern Mediterranean using drifters (2005–2007), Ocean Science, 5, 559–574, https://doi.org/10.5194/os-5-559-2009, 2009.

Gertman, I., Goldman, R., Rosentraub, Z., Ozer, T., Zodiatis, G., Hayes, D., and Poulain, P.: Generation of Shikmona anticyclonic eddy from an alongshore current, in: Rapp. Comm. int. Mer Medit.(CIESM Congress Proceedings), vol. 39, p. 114, 2010.

Goldsmith, S., Krom, M., Sandler, A., and Herut, B.: Spatial trends in the chemical composition of sediments on the continental shelf and slope off the Mediterranean coast of Israel, Continental Shelf Research, 21, 1879–1900, https://doi.org/https://doi.org/10.1016/S0278-4343(01)00027-9, 2001.

Gurgel, K.-W., Antonischki, G., Essen, H.-H., and Schlick, T.: Wellen Radar (WERA): a new ground-wave HF radar for ocean remote sensing, Coastal Engineering, 37, 219–234, https://doi.org/https://doi.org/10.1016/S0378-3839(99)00027-7, 1999.

Gurgel, K.-W., Essen, H.-H., and Schlick, T.: An Empirical Method to Derive Ocean Waves From Second-Order Bragg Scattering: Prospects and Limitations, Oceanic Engineering, IEEE Journal of, 31, 804 – 811, https://doi.org/10.1109/JOE.2006.886225, 2006.

Hasselmann, K.: Determination of Ocean Wave Spectra from Doppler Radio Return from the Sea Surface, Nature Physical Science, 229, 16–17, https://doi.org/10.1038/physci229016a0, 1971.

Herut, B., Krom, M. D., Pan, G., and Mortimer, R.: Atmospheric input of nitrogen and phosphorus to the Southeast Mediterranean: Sources, fluxes, and possible impact, Limnology and Oceanography, 44, 1683–1692, https://doi.org/https://doi.org/10.4319/lo.1999.44.7.1683, 1999.

https://doi.org/10.5194/egusphere-2026-1507
Preprint. Discussion started: 24 March 2026

Herut, B., ALMOGI-LABIN, A., JANNINK, N., and GERTMAN, I.: The seasonal dynamics of nutrient and chlorophyll a concentrations on the SE Mediterranean shelf-slope, Oceanologica Acta, 23, 771–782, https://doi.org/https://doi.org/10.1016/S0399-1784(00)01118-X, 2000.

Ignatiades, L., Gotsis-Skretas, O., Pagou, K., and Krasakopoulou, E.: Diversification of phytoplankton community structure and related parameters along a large east-west transect of the Mediterranean Sea, J. Plankton Res., 31, https://doi.org/10.1093/plankt/fbn124, 2009.

Katz, T., Weinstein, Y., Alkalay, R., Biton, E., Toledo, Y., Lazar, A., Zlatkin, O., Soffer, R., Rahav, E., Sisma-Ventura, G., Bar, T., Ozer, T., Gildor, H., Almogi-Labin, A., Kanari, M., Berman-Frank, I., and Herut, B.: The first deep-sea mooring station in the eastern Levantine basin (DeepLev), outline and insights into regional sedimentological processes, Deep Sea Research Part II: Topical Studies in Oceanography, 171, 104 663, https://doi.org/https://doi.org/10.1016/j.dsr2.2019.104663, revisiting the Eastern Mediterranean: Recent knowledge on the physical, biogeochemical and ecosystemic states and trends (Volume II), 2020.

Kress, N. and Herut, B.: Hypernutrification in the Oligotrophic Eastern Mediterranean: a Study in Haifa Bay (Israel), Estuarine, Coastal and Shelf Science, 46, 645–656, https://doi.org/https://doi.org/10.1006/ecss.1997.0302, 1998.

Kress, N. and Herut, B.: Spatial and seasonal evolution of dissolved oxygen and nutrients in the Southern Levantine Basin (Eastern Mediterranean Sea): chemical characterization of the water masses and inferences on the N:P ratios, Deep Sea Research Part I: Oceanographic Research Papers, 48, 2347–2372, https://doi.org/https://doi.org/10.1016/S0967-0637(01)00022-X, 2001.

Krom, M., Woodward, E., Herut, B., Kress, N., Carbo, P., Mantoura, R., Spyres, G., Thingstad, T., Wassmann, P., Wexels-Riser, C., Kitidis, V., Law, C., and Zodiatis, G.: Nutrient cycling in the south east Levantine basin of the eastern Mediterranean: Results from a phosphorus starved system, Deep Sea Research Part II: Topical Studies in Oceanography, 52, 2879–2896, https://doi.org/https://doi.org/10.1016/j.dsr2.2005.08.009, on the Nature of Phosphorus Cycling and Limitation in the Eastern Mediterranean, 2005.

Krom, M., Emeis, K.-C., and Van Cappellen, P.: Why is the Eastern Mediterranean phosphorus limited?, Progress in Oceanography, 85, 236–244, https://doi.org/https://doi.org/10.1016/j.pocean.2010.03.003, 2010.

Krom, M., Kress, N., Berman-Frank, I., and Rahav, E.: Past, Present and Future Patterns in the Nutrient Chemistry of the Eastern Mediterranean, pp. 49–68, Springer Netherlands, Dordrecht, https://doi.org/10.1007/978-94-007-6704-1_4, 2014.

Krom, M. D., Herut, B., and Mantoura, R. F. C.: Nutrient budget for the Eastern Mediterranean: Implications for phosphorus limitation, Limnology and Oceanography, 49, 1582–1592, https://doi.org/https://doi.org/10.4319/lo.2004.49.5.1582, 2004.

Lorente, P., Aguiar, E., Bendoni, M., Berta, M., Brandini, C., Cáceres-Euse, A., Capodici, F., Cianelli, D., Ciraolo, G., Corgnati, L., Dadić, V., Doronzo, B., Drago, A., Dumas, D., Falco, P., Fattorini, M., Gauci, A., Gómez, R., Griffa, A., Guérin, C.-A., Hernández-Carrasco, I., Hernández-Lasheras, J., Ličer, M., Magaldi, M. G., Mantovani, C., Mihanović, H., Molcard, A., Mourre, B., Orfila, A., Révelard, A., Reyes, E., Sánchez, J., Saviano, S., Sciascia, R., Taddei, S., Tintoré, J., Toledo, Y., Ursella, L., Uttieri, M., Vilibić, I., Zambianchi, E., and Cardin, V.: Coastal high-frequency radars in the Mediterranean – Part 1: Status of operations and a framework for future development, Ocean Science, 18, 761–795, https://doi.org/10.5194/os-18-761-2022, 2022.

Lévy, M., Ferrari, R., Franks, P. J. S., Martin, A. P., and Rivière, P.: Bringing physics to life at the submesoscale, Geophysical Research Letters, 39, https://doi.org/https://doi.org/10.1029/2012GL052756, 2012.

Martin, A.: Phytoplankton patchiness: The role of lateral stirring and mixing, Progress In Oceanography, 57, 125–174, https://doi.org/10.1016/S0079-6611(03)00085-5, 2003.

McWilliams, J. C.: Submesoscale, coherent vortices in the ocean, Reviews of Geophysics, 23, 165–182, https://doi.org/https://doi.org/10.1029/RG023i002p00165, 1985.

https://doi.org/10.5194/egusphere-2026-1507
Preprint. Discussion started: 24 March 2026

Menna, M., Poulain, P.-M., Zodiatis, G., and Gertman, I.: On the surface circulation of the Levantine sub-basin derived from Lagrangian drifters and satellite altimetry data, Deep Sea Research Part I: Oceanographic Research Papers, 65, 46–58, https://doi.org/https://doi.org/10.1016/j.dsr.2012.02.008, 2012.

Mignot, A., Claustre, H., Uitz, J., Poteau, A., D'Ortenzio, F., and Xing, X.: Understanding the seasonal dynamics of phytoplankton biomass and the deep chlorophyll maximum in oligotrophic environments: A Bio-Argo float investigation, Global Biogeochemical Cycles, 28, 856–876, https://doi.org/https://doi.org/10.1002/2013GB004781, 2014.

Morel, A. and Maritorena, S.: Bio-optical properties of oceanic waters: A reappraisal, Journal of Geophysical Research: Oceans, 106, 7163–7180, https://doi.org/https://doi.org/10.1029/2000JC000319, 2001.

Moutin, T., Van Wambeke, F., and Prieur, L.: Introduction to the Biogeochemistry from the Oligotrophic to the Ultraoligotrophic Mediterranean (BOUM) experiment, Biogeosciences, 9, 3817–3825, https://doi.org/10.5194/bg-9-3817-2012, 2012.

Neukermans, G., Reynolds, R., and Stramski, D.: Contrasting inherent optical properties and particle characteristics between an under-ice phytoplankton bloom and open water in the Chukchi Sea, Deep Sea Research Part II: Topical Studies in Oceanography, 105, https://doi.org/10.1016/j.dsr2.2014.03.014, 2014.

Nixon, S. W.: Replacing the Nile: Are anthropogenic nutrients providing the fertility once brought to the Mediterranean by a great river?, Ambio, 32, 30–39, https://doi.org/10.1579/0044-7447-32.1.30, 2003.

Oczkowski, A. J., Nixon, S. W., Granger, S. L., El-Sayed, A.-F. M., and McKinney, R. A.: Anthropogenic enhancement of Egypt's Mediterranean fishery, Proceedings of the National Academy of Sciences, 106, 1364–1367, https://doi.org/10.1073/pnas.0812568106, 2009.

Ozer, T., Gertman, I., Gildor, H., and Herut, B.: Thermohaline Temporal Variability of the SE Mediterranean Coastal Waters (Israel) – Long-Term Trends, Seasonality, and Connectivity, Frontiers in Marine Science, 8, https://doi.org/10.3389/fmars.2021.799457, 2022.

Paulino, A., Heldal, M., Norland, S., and Egge, J.: Elemental stoichiometry of marine particulate matter measured by wavelength dispersive X-ray fluorescence (WDXRF) spectroscopy, Journal of the Marine Biological Association of the United Kingdom, 93, 2003–2014, https://doi.org/10.1017/S0025315413000635, 2013.

Psarra, S., Tselepides, A., and Ignatiades, L.: Primary productivity in the oligotrophic Cretan Sea (NE Mediterranean): seasonal and interannual variability, Progress in Oceanography, 46, 187–204, https://doi.org/https://doi.org/10.1016/S0079-6611(00)00018-5, 2000.

Pujo-Pay, M., Conan, P., Oriol, L., Cornet-Barthaux, V., Falco, C., Ghiglione, J.-F., Goyet, C., Moutin, T., and Prieur, L.: Integrated survey of elemental stoichiometry (C, N, P) from the western to eastern Mediterranean Sea, Biogeosciences, 8, 883–899, https://doi.org/10.5194/bg-8-883-2011, 2011.

Raveh, O., David, N., Rilov, G., and Rahav, E.: The Temporal Dynamics of Coastal Phytoplankton and Bacterioplankton in the Eastern Mediterranean Sea, PLOS ONE, 10, 1–23, https://doi.org/10.1371/journal.pone.0140690, 2015.

Reich, T., Ben-Ezra, T., Belkin, N., Tsemel, A., Aharonovich, D., Roth-Rosenberg, D., Givati, S., Bialik, M., Herut, B., Berman-Frank, I., Frada, M., Krom, M. D., Lehahn, Y., Rahav, E., and Sher, D.: A year in the life of the Eastern Mediterranean: Monthly dynamics of phytoplankton and bacterioplankton in an ultra-oligotrophic sea, Deep Sea Research Part I: Oceanographic Research Papers, 182, 103 720, https://doi.org/https://doi.org/10.1016/j.dsr.2022.103720, 2022.

Ribera d'Alcalà, M., Civitarese, G., Conversano, F., and Lavezza, R.: Nutrient ratios and fluxes hint at overlooked processes in the Mediterranean Sea, Journal of Geophysical Research: Oceans, 108, https://doi.org/https://doi.org/10.1029/2002JC001650, 2003.

Robinson, A. R. and Golnaraghi, M.: The physical and dynamical oceanography of the Mediterranean Sea, in: Ocean processes in climate dynamics: Global and Mediterranean examples, pp. 255–306, Springer, 1994.

https://doi.org/10.5194/egusphere-2026-1507
Preprint. Discussion started: 24 March 2026

Rosentraub, Z. and Brenner, S.: Circulation over the southeastern continental shelf and slope of the Mediterranean Sea: Direct current measurements, winds, and numerical model simulations, Journal of Geophysical Research: Oceans, 112, https://doi.org/10.1029/2006jc003775, 2007.

Rubin-Blum, M., Sisma-Ventura, G., Yudkovski, Y., Belkin, N., Kanari, M., Herut, B., and Rahav, E.: Diversity, activity, and abundance of benthic microbes in the Southeastern Mediterranean Sea, FEMS Microbiology Ecology, 98, fiac009, https://doi.org/10.1093/femsec/fiac009, 2022.

Siokou-Frangou, I., Christaki, U., Mazzocchi, M. G., Montresor, M., Ribera d'Alcalá, M., Vaqué, D., and Zingone, A.: Plankton in the open Mediterranean Sea: a review, Biogeosciences, 7, 1543–1586, https://doi.org/10.5194/bg-7-1543-2010, 2010.

Teruzzi, A., Bolzon, G., Feudale, L., and Cossarini, G.: Deep chlorophyll maximum and nutricline in the Mediterranean Sea: emerging properties from a multi-platform assimilated biogeochemical model experiment, Biogeosciences, 18, 6147–6166, https://doi.org/10.5194/bg-18-6147-2021, 2021.

van Leeuwen, S. M., Beecham, J. A., García-García, L. M., and Thorpe, R.: The Mediterranean Rhodes Gyre: modelled impacts of climate change, acidification and fishing, Marine Ecology Progress Series, 690, pp. 31–50, https://www.jstor.org/stable/27179442, 2022.

Verma, V., Barkan, R., Solodoch, A., Gildor, H., and Toledo, Y.: The Eastern Mediterranean Boundary Current: Seasonality, Stability, and Spiral Formation, Journal of Physical Oceanography, 54, 1971–1989, https://doi.org/10.1175/jpo-d-23-0207.1, 2024.

Volpe, G., Buongiorno Nardelli, B., Colella, S., Pisano, A., and Santoleri, R.: An Operational Interpolated Ocean Colour Product in the Mediterranean Sea, https://doi.org/10.17125/gov2018.ch09, 2018.

Volpe, G., Colella, S., Brando, V., Forneris, V., Padula, F., Di Cicco, A., Sammartino, M., Bracaglia, M., Artuso, F., and Santoleri, R.: The Mediterranean Ocean Colour Level 3 Operational Multi-Sensor Processing, Ocean Science Discussions, pp. 1–26, https://doi.org/10.5194/os-2018-73, 2019.

Wang, Y., Zhang, H.-R., Chai, F., and Yuan, Y.: Impact of mesoscale eddies on chlorophyll variability off the coast of Chile, PLOS ONE, 13, 1–13, https://doi.org/10.1371/journal.pone.0203598, 2018.

Wyatt, L.: High-frequency radar measurements of the ocean wave-directional spectrum, IEEE Journal of Oceanic Engineering, 16, 163–169, https://doi.org/10.1109/48.64896, 1991.

Xu, W., Wang, G., Cheng, X., Xing, X., Qin, J., Zhou, G., Jiang, L., and Chen, B.: Mesoscale Eddy Modulation of Subsurface Chlorophyll Maximum Layers in the South China Sea, Journal of Geophysical Research: Biogeosciences, 128, e2023JG007 648, https://doi.org/https://doi.org/10.1029/2023JG007648, e2023JG007648 2023JG007648, 2023.

Zeng, L. and Li, D.: Development of In Situ Sensors for Chlorophyll Concentration Measurement, Journal of Sensors, 2015, 903 509, https://doi.org/https://doi.org/10.1155/2015/903509, 2015.

Zodiatis, G., Brenner, S., Gertman, I., Ozer, T., Simoncelli, S., Ioannou, M., and Savva, S.: Twenty years of in-situ monitoring in the south-eastern Mediterranean Levantine basin: Basic elements of the thermohaline structure and of the mesoscale circulation during 1995-2015, Frontiers in Marine Science, Volume 9 - 2022, https://doi.org/10.3389/fmars.2022.1074504, 2023.

Zohary, T. and Robarts, R. D.: Experimental study of microbial P limitation in the eastern Mediterranean, Limnology and Oceanography, 43, 387–395, https://doi.org/https://doi.org/10.4319/lo.1998.43.3.0387, 1998.